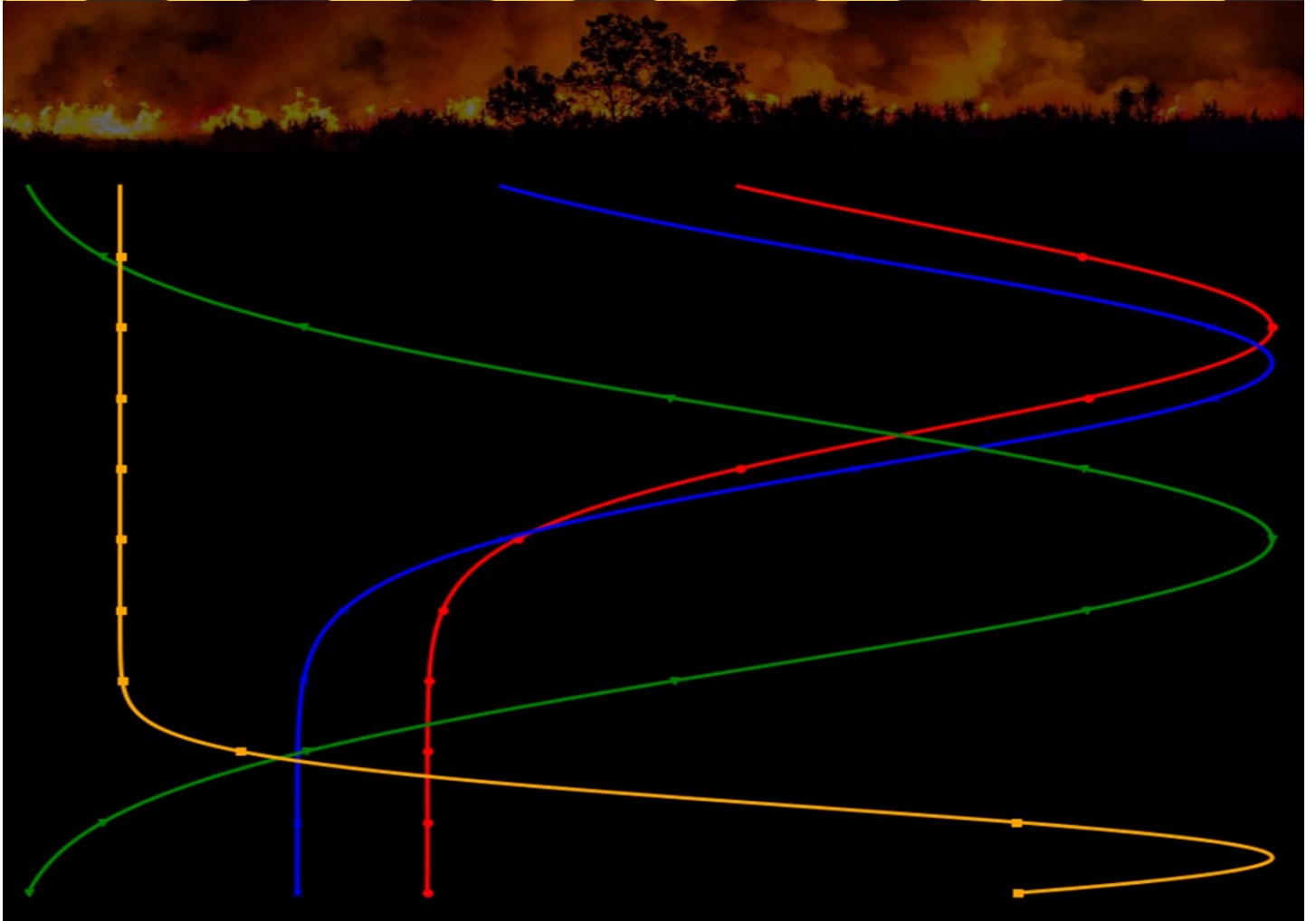


[bnhcrc.com.au](http://bnhcrc.com.au)

# STUDYING LEAF AREA DENSITY BASED WIND ADJUSTMENT FACTOR IN SPARK

**Mahmood Rashid & Khalid Moinuddin**

Victoria University & Bushfire and Natural Hazards CRC





Version	Release history	Date
1.0	Initial release of document	22/11/2021



**Australian Government**  
Department of Industry, Science,  
Energy and Resources

**AusIndustry**  
Cooperative Research  
Centres Program

© 2021 Bushfire and Natural Hazards CRC

All material in this document, except as identified below, is licensed under the Creative Commons Attribution-Non-Commercial 4.0 International Licence.

Material not licensed under the Creative Commons licence:

- Department of Industry, Science, Energy and Resources logo
- Cooperative Research Centres Program logo
- Bushfire and Natural Hazards CRC logo
- Any other logos
- All photographs, graphics and figures

All content not licenced under the Creative Commons licence is all rights reserved. Permission must be sought from the copyright owner to use this material.



**Disclaimer:**

Victoria University and the Bushfire and Natural Hazards CRC advise that the information contained in this publication comprises general statements based on scientific research. The reader is advised and needs to be aware that such information may be incomplete or unable to be used in any specific situation. No reliance or actions must therefore be made on that information without seeking prior expert professional, scientific and technical advice. To the extent permitted by law, Victoria University and the Bushfire and Natural Hazards CRC (including its employees and consultants) exclude all liability to any person for any consequences, including but not limited to all losses, damages, costs, expenses and any other compensation, arising directly or indirectly from using this publication (in part or in whole) and any information or material contained in it.

**Publisher:**

Bushfire and Natural Hazards CRC

November 2021

Citation: Rashid M & Moinuddin K (2021) Studying leaf area density based wind adjustment factor in Spark, Bushfire and Natural Hazards CRC, Melbourne.



## **TABLE OF CONTENTS**

---

<b>ACKNOWLEDGMENTS</b>	<b>4</b>
<b>EXECUTIVE SUMMARY</b>	<b>5</b>
<b>END-USER STATEMENT</b>	<b>6</b>
<b>INTRODUCTION</b>	<b>7</b>
<b>MODEL DESCRIPTION</b>	<b>9</b>
<b>RESEARCH APPROACH</b>	<b>13</b>
<b>PRELIMINARY RESULTS BASED ON SYNTHETIC DATA</b>	<b>14</b>
<b>ASSESSMENT USING ACTUAL CASE STUDIES</b>	<b>17</b>
Selected cases	17
Parametric variations	18
<b>RESULTS AND DISCUSSIONS</b>	<b>19</b>
<b>CONCLUSIONS</b>	<b>23</b>
<b>REFERENCES</b>	<b>24</b>



## **ACKNOWLEDGMENTS**

We would like to acknowledge the contribution of Dr Duncan Sutherland of UNSW, Canberra in interpreting the equations towards implementing them in Spark. We also acknowledge Dr James Hilton of CSIRO Data61 for assisting us to use Spark.



## EXECUTIVE SUMMARY

In some operational fire prediction models such as the McArthur model [1] or Vesta model [2], a static (constant) wind reduction factor (WRF) is used to account for subcanopy wind profile. However, the WRF is far more complicated than what can be described by a constant value. A dynamic WRF depends on wind velocity well above the forest canopy, canopy height and canopy density which may vary from location to location. In our earlier work, we developed a simpler model considering uniform vertical canopy density, known as the Harman-Finnigan model [3]. However, Moon et al. [4] and Sutherland et al. [5] demonstrated that vertically heterogenous leaf area density (LAD) can significantly change the WRF. Massman et al [6] presented a set of equations accounting for vertically heterogenous LAD, plant area index (PAI) and above-canopy wind profiles towards calculating subcanopy wind adjustment factor (WAF). WAF is basically the inverse of WRF. In this study, we implement this LAD based WRF (by inverting Massman's WAF) model in CSIRO's Spark platform within its Vesta fire propagation model [2].

This research was initially tested using a synthetic dataset to apply canopy parameters that represent Australian vegetation properties. The preliminary Spark simulation results show some variation in fire rate of spread based on various vegetation types. Further, we assess the implementation using three case studies based on three fire incidents, Mount Cooke Fire 2003 of Western Australia, Kilmore Fire 2009 of Victoria, and Lithgow Fire (State Mine) 2013 of New South Wales. Taking PAI as half of leaf area index (LAI), testing four different LAD configurations, it is found that for Tall Open Eucalyptus LAD, best results are obtained in relation to actual final fire perimeters.



## END-USER STATEMENT

**Dr James Hilton**, *Principal Research Scientist, CSIRO Data-61*

Wind reduction factors (WRF) are usually estimated or applied as a constant value over a particular fuel type in wildfire prediction. However, the effect of vegetation on wind is a complex process dependent on factors including vegetation condition, canopy height, fuel sparsity or patchiness. This, in turn, affects fire predictions, as wind is a key factor in all wildfire rate-of-spread models. The use of constant or estimated WRF is partially due to the difficulty in spatial assessment of WRF over wide areas, particularly in a consistent way. This work represents an important step forward in addressing these issues and implementing and testing a physically based spatial WRF model in a wildfire modelling system. The processing can be based on remote sensed data and automatically converted in the required WRF data, which would be suitable for scaling for use on a national scale for wildfire prediction.

## INTRODUCTION

Understanding the behaviour of bushfires is essential for fire management authorities to effectively minimise losses of properties and lives. Proper scheduling of supply chain and logistics to the affected areas is highly dependent on the prediction of the behaviour of the fire and the rate of spread (RoS). Fire behaviour is governed by various parameters on the affected locality. Factors, such as localised topography, weather conditions, vegetation, and terrain have varying ranges of influences on RoS, which makes prediction highly complex. Currently, RoS predictions are achieved by simple operational models that have the useful attribute of providing results on time scales commensurate with the requirements of emergency managers. In the case of forest fires, canopies play important roles by reducing the wind velocity throughout the height of the flames. In most operational fire prediction models such as McArthur or Vesta model [1] [2], a static (constant) wind reduction factor (WRF) is used to account for the effect of forest canopies.

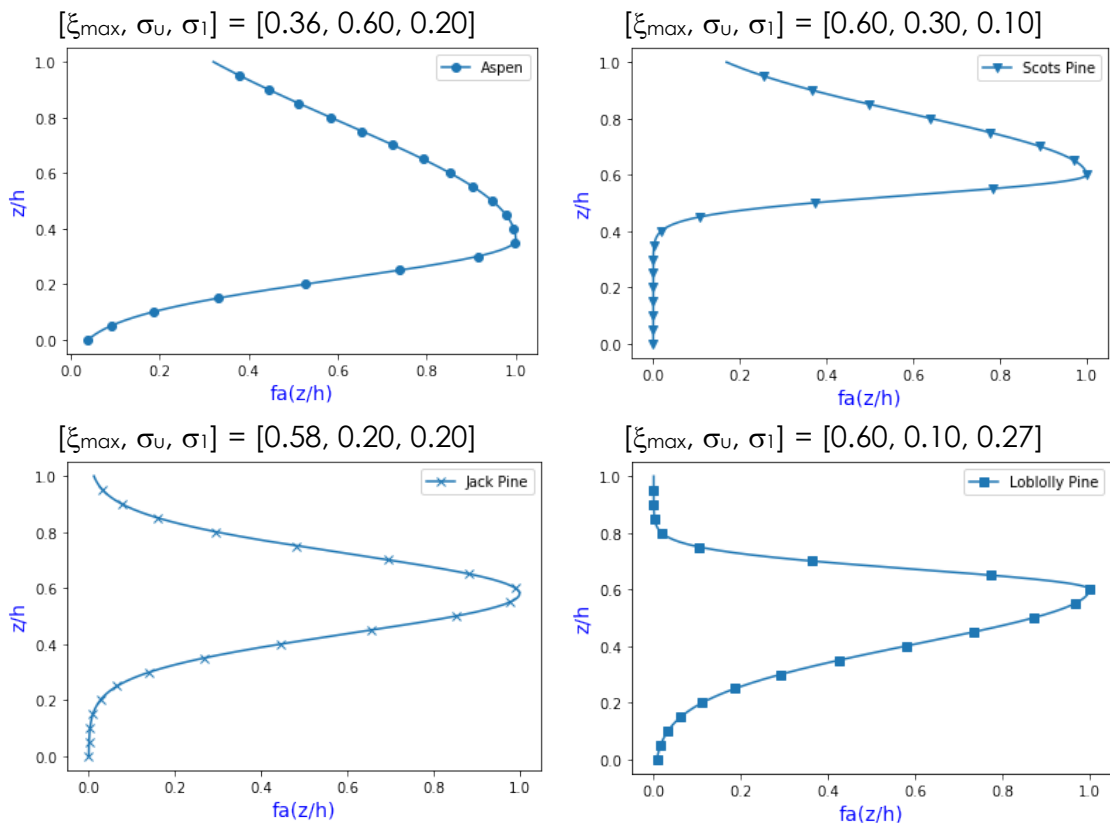


FIG. 1 THE FOLIAGE DISTRIBUTION SHAPE FOR ASPEN, SCOTS PINE, JACK PINE, AND LOBLOLLY PINE CANOPIES FITTED WITH ASYMMETRIC GAUSSIAN MODEL.

We previously developed a plugin based on relatively simple dynamic WRF proposed by Harman and Finnigan [3]. It has been implemented in CSIRO's operational model, Spark [7]. A dynamic WRF varies from location to location based on wind velocity well above the forest canopy, canopy height and canopy density. The Harman and Finnigan [3] model assumes that the canopy density (known as leaf area density, LAD) is vertically uniform. However, research shows that vertically heterogenous LAD can significantly change the WRF [4] [5]. Massman et al [6] proposed a set of equations accounting for vertically heterogenous LAD and above canopy wind profiles to determine the



subcanopy wind adjustment factor (WAF), which is basically the inverse of WRF. Massman et al. applied their model for the foliage distribution shape presented in Figure 1, which is based on American forest standards based on Equation (7) (see the **Understanding and Translating the Model** section).

In this work, we intend to implement Massman et al.'s LAD based dynamic WRF model in CSIRO's operational model, Spark [7] and test at first, synthetic data, then actual fire data applying canopy parameters that represent Australian vegetation properties.



## MODEL DESCRIPTION

The Massman et al. [6] model computes WAF at a single point in parameter space. That is the WAF is not a function of height within the canopy. Instead, the 'height' where WAF is computed is the half flame height. Flame height is an input parameter to the model, so it would be possible to compute a range of WAF through custom inputs as per the fire behaviour analyst's choice of flame height.

We computationally solved a series of equations towards implementing the Massman model. Table 1 represents the list of Massman equations numbers with their dependencies along with the corresponding variables calculated by those equations.

Massman Equation	Values looking for	Definition	Dependent Variables	Massman Equation/s
17	$WAF_{sub}$	Subcanopy wind adjustment factor	$U_b(\xi), U_t(\xi), d/h, z_0/h$	6, 7, 15, 16
6	$U_b(\xi)$	Logarithmic wind speed which is dominant near the ground and the lower part of the canopy	Independent	
7	$U_t(\xi)$	Hyperbolic cosine wind speed which dominates near the top of the canopy	$\zeta(h), \zeta(\xi), N$	4, 5, 8
4	$\zeta(h)$	The drag area index	$ha(\xi), c_d(\xi)$	1, 3
1	$ha(\xi)$	Plant surface distribution function	$f_a(\xi)$	2
2	$f_a(\xi)$	An arbitrary function for $0 \leq \xi \leq 1$ (i.e., $0 \leq z \leq h$ ) that describes the desired mathematical shape of the plant surface distribution	Independent	
3	$c_d(\xi)$	Bulk drag coefficient	$ha(\xi)$	1
5	$\zeta(\xi)$	The cumulative drag area	$ha(\xi), c_d(\xi)$	1, 3
8	$N$	(The drag area index)/(The surface drag coefficient)	$\zeta(h), C_{surf}$	4, 9
9	$C_{surf}$	The surface drag coefficient	$u^*(h)/u(h)$	10
10	$u^*(h)/u(h)$		$\zeta(h)$	4
15	$d/h$	$\frac{\text{Displacement height}}{\text{Canopy height}}$	$u^2(\xi)/u^2(1)$	12
12	$u^2(\xi)/u^2(1)$		$\zeta(h), \zeta(\xi), N, C_{surf}$	4, 5, 8, 9
16	$z_0/h$	$\frac{\text{Vegetation roughness length}}{\text{displacement height}}$	$C_{surf}, u^*(h)/u(h), d/h$	9, 10, 15

TABLE 1. THEIR DEPENDENCIES AMONG THE MASSMAN EQUATIONS.

As the wind reduction factor is the inverse of the wind adjustment factor, we apply Equation (1) to calculate the subcanopy wind reduction factor,  $WRF_{sub}$ .

$$WRF = \frac{1}{WAF_{sub}} \dots \dots \dots (1)$$



Subcanopy wind adjustment factor,  $WAF_{sub}$  is calculated using Equation (2) which is the objective of the model. However, to solve Equation (2) we need to solve a series of equations as stated below through Equations (3) to Equation (15). Note that the terms used in these equations are defined in Table 1 and Table 2.

$$WAF_{sub} = U_b(\xi_{mid}) U_t(\xi_{mid}) \frac{\ln\left(\lambda_{rs} \left[\frac{1-d/h}{z_0/h}\right]\right)}{\ln\left(\lambda_{rs} \left[\frac{H/h + 1 - d/h}{z_0/h}\right]\right)} \dots \dots \dots (2)$$

$$U_b(\xi) = \begin{cases} \frac{\log(z/z_{0G})}{\log(h/z_{0G})} = \frac{\log(z/z_{0G})}{\log(1/\xi_{0G})} & z_{0G} \leq z \leq h \\ 0, & 0 \leq z \leq z_{0G} \end{cases} \dots \dots \dots (3)$$

$$U_t(\xi) = \frac{\cosh[N\zeta(\xi)/\zeta(h)]}{\cosh(N)} \quad 0 \leq z \leq h \dots \dots \dots (4)$$

$$\zeta(h) \equiv \int_0^h C_d(\xi') ha(\xi') d\xi' \dots \dots \dots (5)$$

$$ha(\xi) = PAI \frac{f_a(\xi)}{\int_0^1 f_a(\xi') d\xi'} \dots \dots \dots (6)$$

$$f_a(\xi) = \begin{cases} \exp\left(-\frac{(\xi_{max} - \xi)^2}{\sigma_1^2}\right) & 0 \leq \xi \leq \xi_{max} \end{cases} \dots \dots \dots (7)$$

$$C_d(\xi) = C_d \left[ \frac{e^{-d_1(1-\xi)}}{1 + p_1 ha(\xi)} \right] \dots \dots \dots (8)$$



$$\frac{d}{h} = \left(1 - \frac{u_*^2(0)}{u_*^2(1)}\right) \frac{\int_0^1 [u_*^2(\xi)/u_*^2(1)] \xi d\xi}{\int_0^1 [u_*^2(\xi)/u_*^2(1)] d\xi} \quad \dots \dots \dots \quad (9)$$

$$\zeta(\xi) = \int_0^\xi C_d(\xi') h a(\xi') d\xi' \quad \dots \dots \dots \quad (10)$$

$$N = \frac{\zeta(h)}{C_{surf}} \quad \dots \dots \dots \quad (11)$$

$$C_{surf} = \frac{2u_*^2(h)}{u^2(h)} \quad \dots \dots \dots \quad (12)$$

$$\frac{u_*(h)}{u(h)} = c_1 - c_2 \exp[-c_3 \zeta(h)] \quad \dots \dots \dots \quad (13)$$

$$\frac{u_*^2(\xi)}{u_*^2(1)} = \frac{\cosh[q_* N \zeta(\xi)/\zeta(h)]}{\cosh(q_* N)} \quad \text{for } 0 \leq z \leq h \quad \dots \dots \dots \quad (14)$$

$$\frac{z_0}{h} = \lambda_{rs} \left(1 - \frac{d}{h}\right) e^{-\frac{k}{[u_*(h)/u(h)]}} = \lambda_{rs} \left(1 - \frac{d}{h}\right) e^{-k \sqrt{2/C_{surf}}} \quad \dots \dots \dots \quad (15)$$

The above equations require a number of input parameters. Table 2 presents the model parameters that have both constants and input variables. The first four constants are based on experimental observations and are kept unchanged during all simulations. Canopy height and plant area index (PAI) data at various geographical locations can be obtained from Landscape Data Visualiser [8].  $\xi_{max}$ ,  $\sigma$  and *shift* together represent the shape of the LAD profiles.

Parameter	Definition	Type
$\kappa=0.4$	von Karmann constant	Constant
$\xi_{0G} = 0.0025$	Fundamental roughness length	Constant
$\lambda_{rs}=1.25$	Parameter in an exponential	Constant
$C_d = 0.15$	Drag Coefficient	Constant
$\xi$	$\xi = z/h$ in which z and h denote the vertical height	Model input -



	above the ground and the canopy height, respectively.	variable
<b>h</b>	<b>Canopy Height</b>	<b>Model input - variable</b>
<b>PAI</b>	<b>Plant Area Index</b>	<b>Model input - variable</b>
$\xi_{max}$	Location of the maximum plant density	Model input - constant
$\sigma_L$	Width of piecewise Gaussian in the lower canopy	Model input - constant
$\sigma_U$	Width of piecewise Gaussian in the upper canopy	Model input - constant
Shift	Horizontal shift of the reference point from (0,0)	Model input - constant
<b>h<sub>f</sub></b>	<b>Flame height – either provided as input or calculated from the canopy height, h</b>	<b>Model input - variable</b>
$h_{REF}$	Wind measurement location	Model input - constant
$H = h_{REF} - h$	Height from top of the canopy to the measurement location	Model input - constant

TABLE 2. MODEL PARAMETERS.

## RESEARCH APPROACH

To implement the model, we have selected four vertically heterogeneous LAD profiles of Australian forest from Moon et al. [4]. Sutherland et al. [5] mathematically fitted LAD profiles of these four Australian forests. The relevant parameter values ( $\xi_{max}, \sigma, shift$ ) and derived the vertical LAD shapes are shown in Figure 2.

As the model only computes at single points in parameter space, it will compute only one WAF on mid-flame height either within subcanopy (sheltered) or above the canopy. We can generate a WAF profile by computing over a forest height with the incremental flame-height ( $h_f$ ). Each profile will have WAF values of subcanopy and above the canopy. Then we relate the WAF to the WRF, which is usually just an inverse relationship but may be different for the above canopy WAF. In the current version of Spark, only one wind adjustment factor is applicable and hence, we are focusing on the subcanopy WAF in our preliminary implementation. The four WRF profiles based on four LAD profiles presented in Figure 2 are shown in Figure 3. The WRFs were then used within the Vesta fire propagation empirical model of Spark.

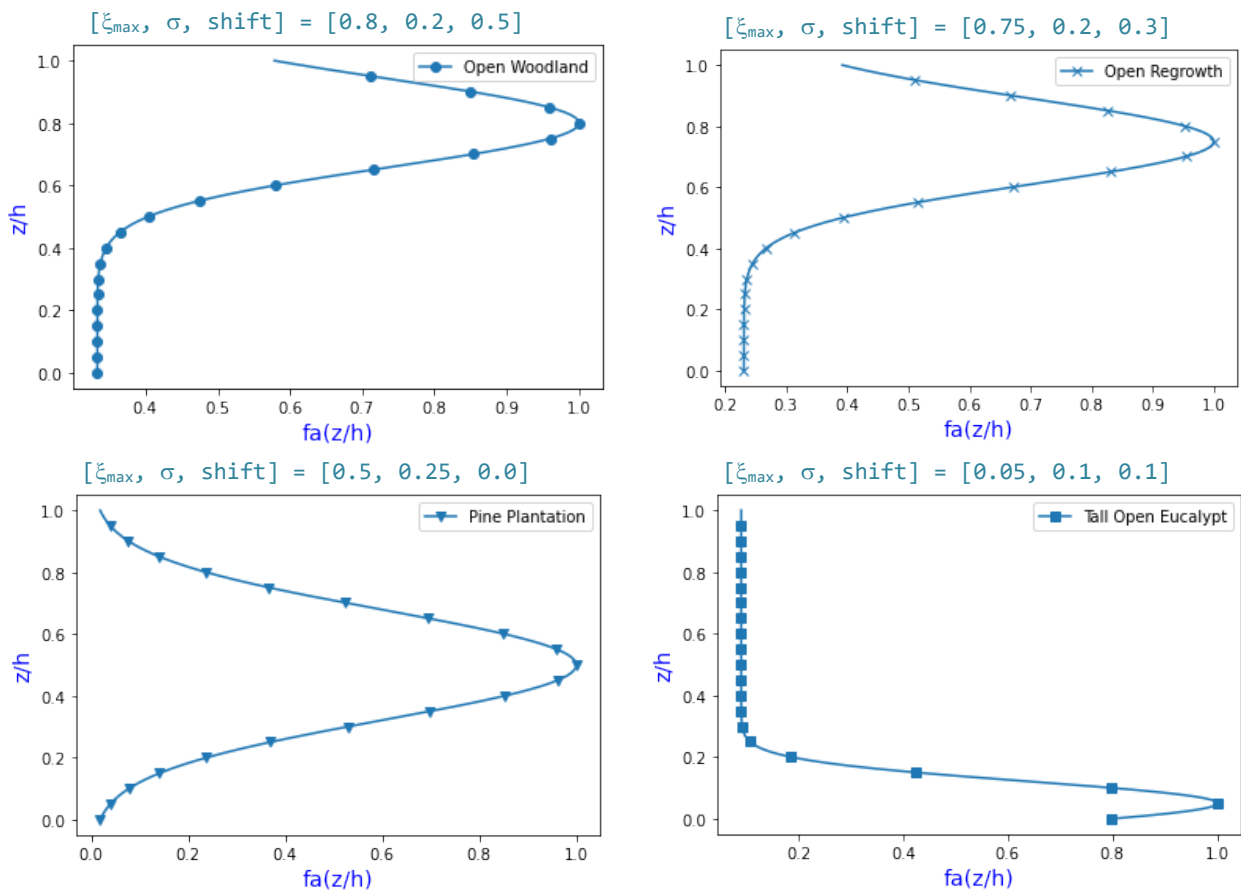


FIG. 2 THE VERTICAL LAD DISTRIBUTION SHAPE FOR AUSTRALIAN FORESTS, OPEN WOODLAND, OPENREGROWTH, PINE PLANTATION, AND TALL OPEN EUCALYPT FITTED WITH PIECE-WISE GAUSSIAN MODEL.

## PRELIMINARY RESULTS BASED ON SYNTHETIC DATA

A point ignition is modelled at [longitude, latitude] = [150.167°, -33.679°]. At this location leaf area index (LAI) is 2.7. LAI is closely related to PAI. Based on this LAI, LADs are varied into four different shapes as per Figure 2. For simplicity, instead of variable LAI (at different locations), a fixed LAI of 2.7 is considered. Flame height is taken at 20 m and the corresponding WRF is taken from Figure 3.

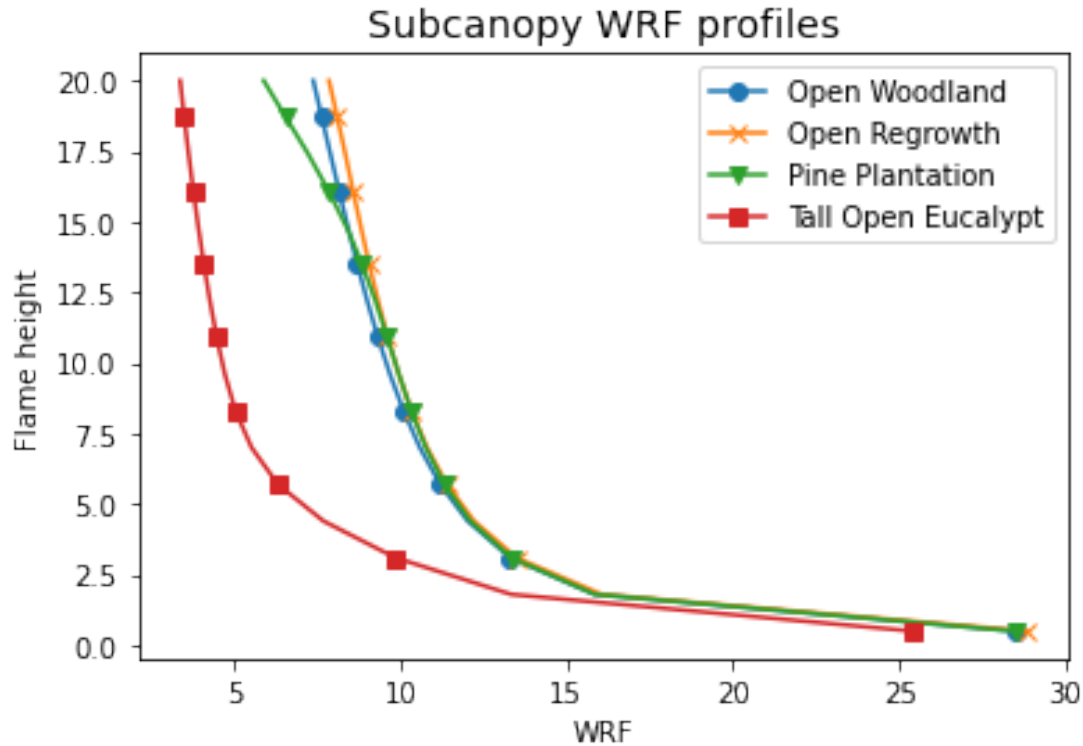
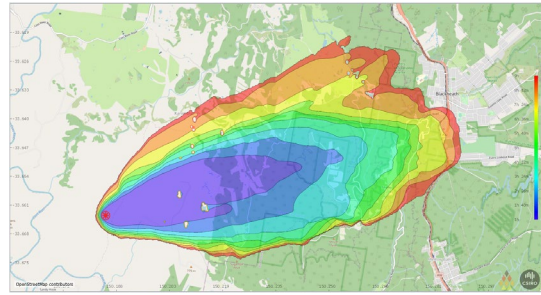
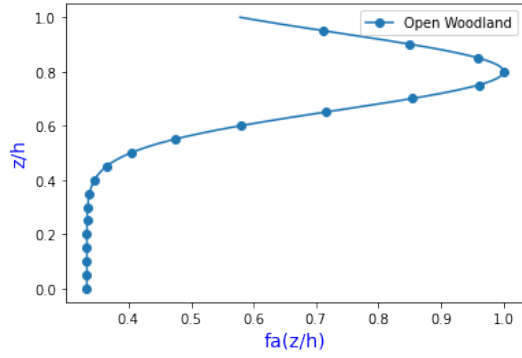


FIG. 3 WRF PROFILE WITH VARYING  $H_f$  FOR FOUR AUSTRALIAN FOREST TYPES APPLYING MOON'S VERTICAL LAD PROFILES.

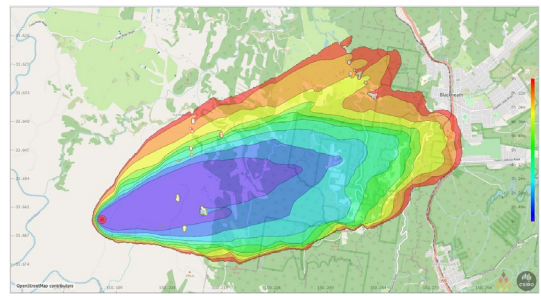
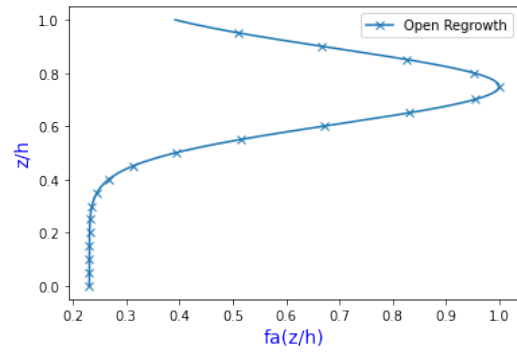
The extent of fire propagation at various times are presented in Figure 4. The LAD profiles of open woodland and open regrowth show that for this type of forest the canopy is denser in the upper portion and are very similar in shape. As a result, WRF profiles are also very similar (see Figure 3). The propagation for these two profiles is very similar as shown in the top two cases of Figure 4 (Open Woodland and Open Regrowth).

For pine plantation, the denser portion is at the middle of the height which leads to generating the similar WRF as woodland and regrowth forests (except at the very top) and the propagation is quite similar. However, for open eucalypt, the denser portion is at the bottom and hence it generates a small WRF at the top due to a less dense canopy which leads the fire to propagate more as shown in the last case of Figure 4 (d).

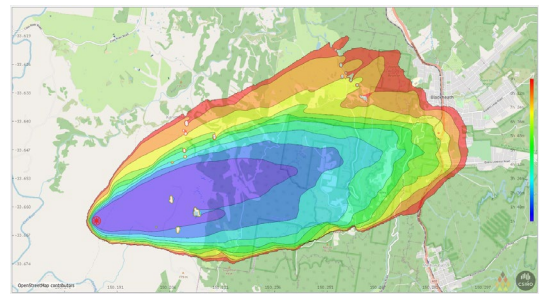
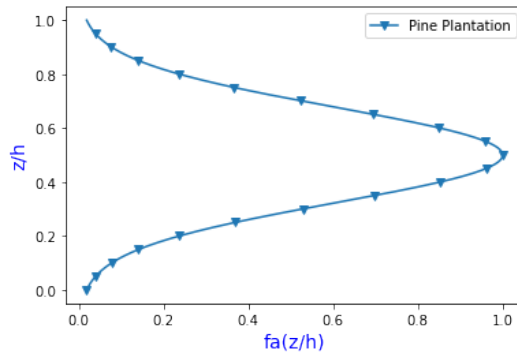
We also compare the propagation for the profiles as shown in Figure 5. In the case of open eucalypt forest, the fire propagates far more than that of the others. We have shown that considering the same LAI and flame height, different LAD profiles can lead to different extent of fire propagation.



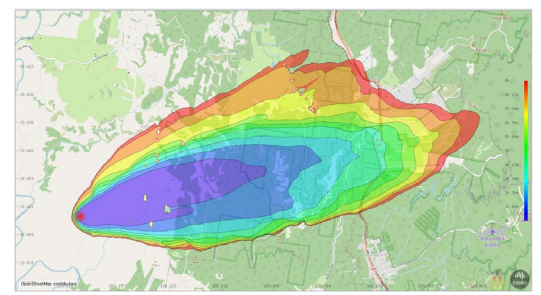
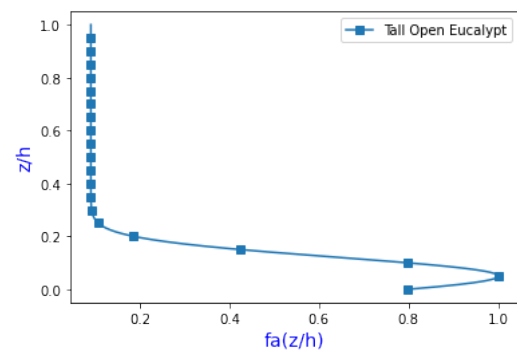
(a) Flame-height=20; LAI=2.7 WRF=4.84



(b) Flame-height=20; LAI=2.7 WRF=5.03



(c) Flame-height=20; LAI=2.7 WRF=4.26



(d) Flame-height=20; LAI=2.7 WRF=2.92

FIG. 4 LAD PROFILE BASED FIRE PROPAGATION FOR FOUR DIFFERENT AUSTRALIAN FOREST TYPES, OPEN WOODLAND, OPEN REGROWTH, PINE PLANTATION AND TALL OPEN EUCALYPT.

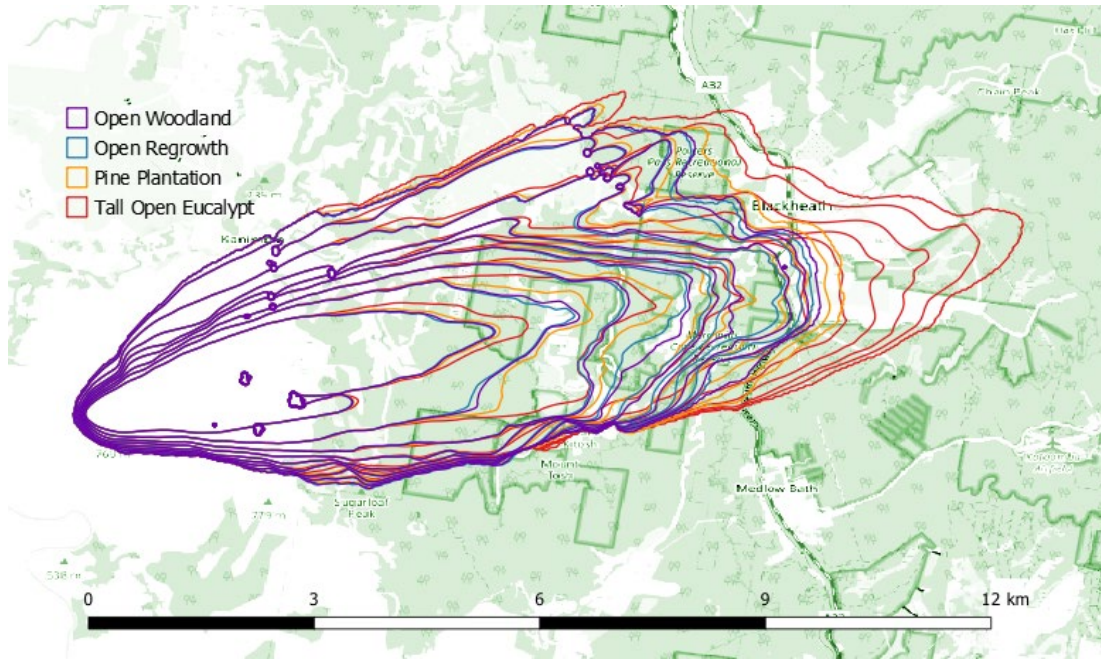


FIG. 5 COMPARISON OF FIRE PROPAGATION BASED ON VERTICAL LAD PROFILE DERIVED FROM MOON'S VERTICAL WIND PROFILE.

## ASSESSMENT USING ACTUAL CASE STUDIES

### SELECTED CASES

To assess the effectiveness of LAD based WRF, we run our model on the following three cases:

- **Kilmore Fire 2009 of Victoria:** The ignition time was approximately 11:45 am on 7 February caused by a power line spark. The fire was fanned by extreme northwesterly wind, and travelled around 50 km southeast with a narrow fire front [9].
- **Lithgow Fire 2013 of New South Wales:** The State Mine fire started as a minor fire on 16 October 2013 near a defence force training base at Marrangaroo, and travelled up to 25 kilometres on 17 October. The fire burnt out more than 55,000 hectares between Lithgow and Bilpin [10].
- **Mount Cooke 2003 of Western Australia:** On a warm, dry day in January 2003 a lightning strike sparked a wildfire at Mt Cooke. It burnt through more than 18,000 hectares over three days, making it one of the largest wildfires ever recorded in the northern jarrah forest [11].

We calculated the dynamic WRF based on the recorded LAI of the previous years of the incidents of the respective cases. We extracted the LAI of the affected areas bounded by the longitudes and latitudes of those regions. First, we downloaded the LAI data from the landscape visualizer [8] and then extracted the LAI data for the fire affected area. Similarly, vegetation height data was extracted from Australian vegetation data [12] to generate a height raster map to use as input in Spark. LAI and height raster maps for the Lithgow area are shown in Figure 6, as an example to calculate WRF using our mathematical model.

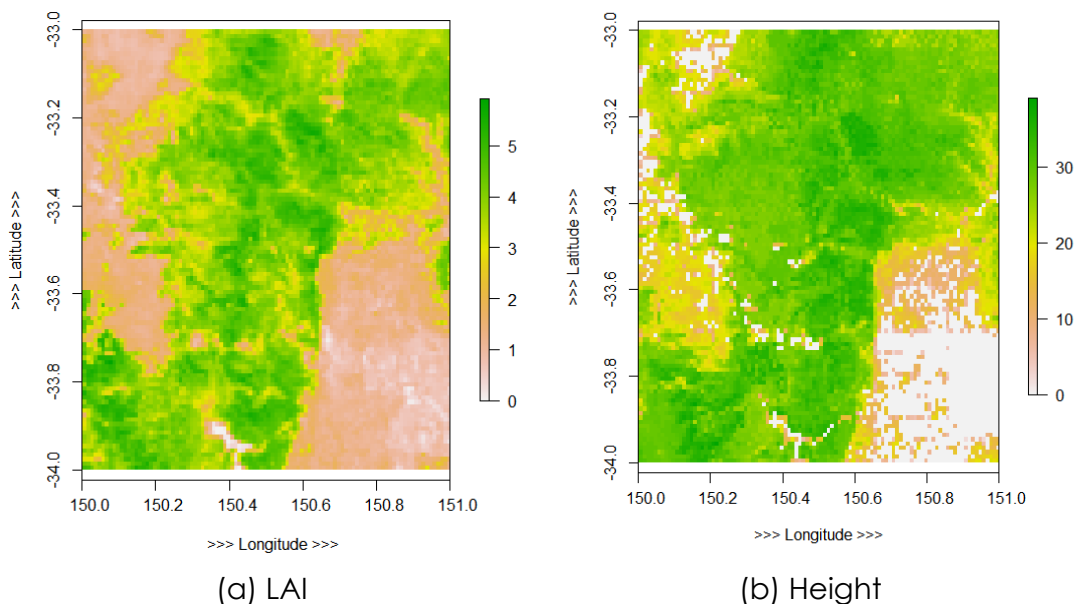


FIG. 6 THE FIGURES (A) AND (B) RESPECTIVELY REPRESENT THE LAI AND THE CANOPY HEIGHT RASTER MAPS OF THE 2013 LITHGOW FIRE, NSW INCIDENT AREA.



## PARAMETRIC VARIATIONS

Two parameters have been varied to understand the effects of these two parameters (1) determination of PAI and (2) WRF for cells where no LAI and/or  $H$  data is available.

As shown in Figure 6, we have access to the LAI data. However, the PAI data is not available. Comparing the PAI data presented by Moon et al. [4] and the LAI data from landscape visualizer [8] at the same location, it appears that for the open woodland LAI and PAI values are the same. However, for other forests  $PAI \cong LAI/2$ . Therefore, we conducted our studies for both PAI = LAI and PAI = LAI/2.

When no vegetation is found in cells, there is uncertainty as to whether actual vegetation exists or there is difficulty in measuring LAI and  $H$ . Therefore, two simulations are conducted: (1) With the default WRF = 3.0 considering that the empirical WRF value was obtained using the fire progression over a large landscape and (2) With WRF=1, considering that actually no vegetation exists. For the selection of WRF=1.0, it is to be noted that once wind emerges to a cell of no vegetation, the wind profile will not immediately recover to an open-wind profile.

## RESULTS AND DISCUSSIONS

The study results are presented in Figures 7, 8 and 9. Different contour colours are used for the hourly fire perimeter from simulations with various LADs. We have also presented the results using the Base Spark (where  $WRF=3.0$  throughout). The black dotted line represents the actual final fire perimeter recorded.

Based on the results of the Kilmore fire (Figure 7), we found that for  $PAI = LAI$ , the fire spread for all of the LAD profile based simulations underperformed in comparison to the fire spread of the Base Spark regardless of the default WRF values. On the other hand, for  $PAI = LAI/2$ , the LAD based simulations performed better in comparison to the fire spread of the Base Spark regardless of the default WRF values. Note that among the LAD profiles, *Tall Open Eucalyptus* is performing better than others. Cruz et al [9] reported that the Kilmore fire had significant eucalyptus plantation and low understorey fuel type was the predominant fuel in terms of burn severity. Based on this the LAD shape was very likely to be *Tall Open Eucalyptus* type. Cruz et al also reports the effect of ember transport and ignition by embers which are not modelled in the simulations.

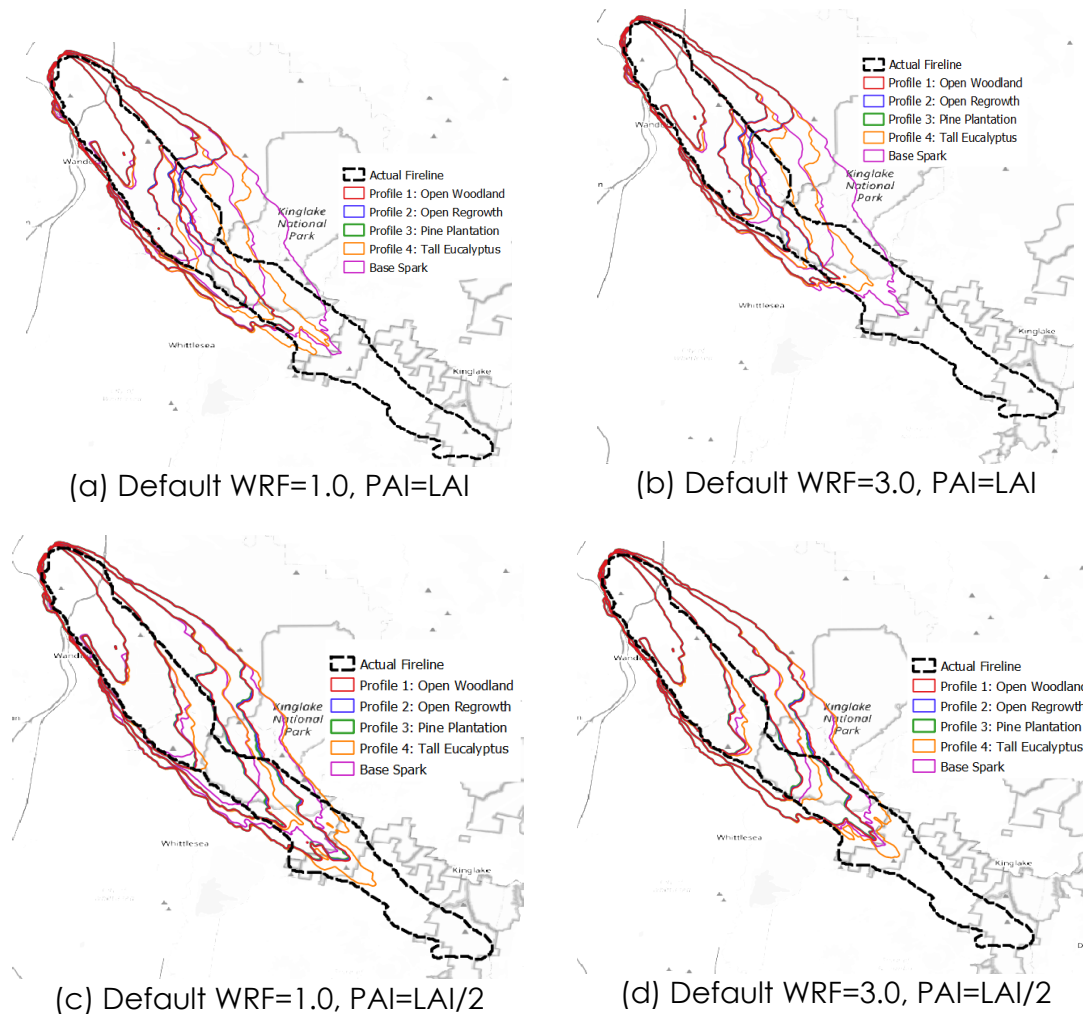
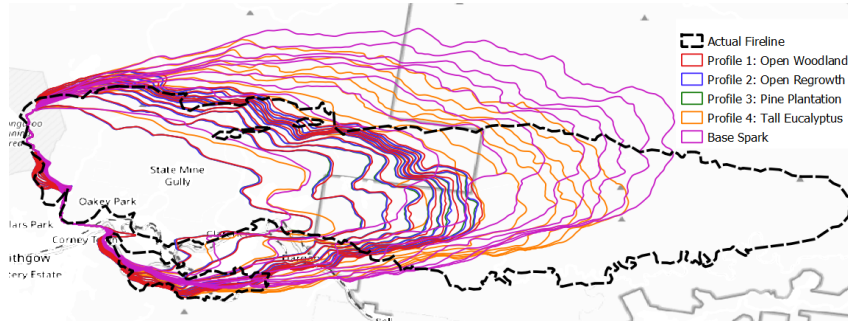
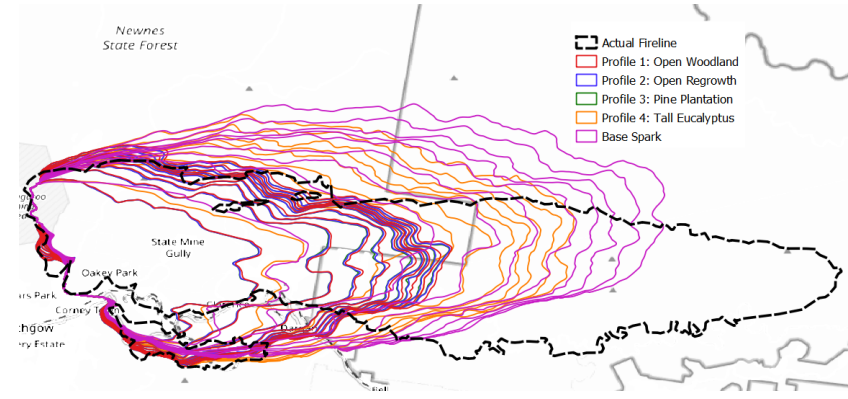


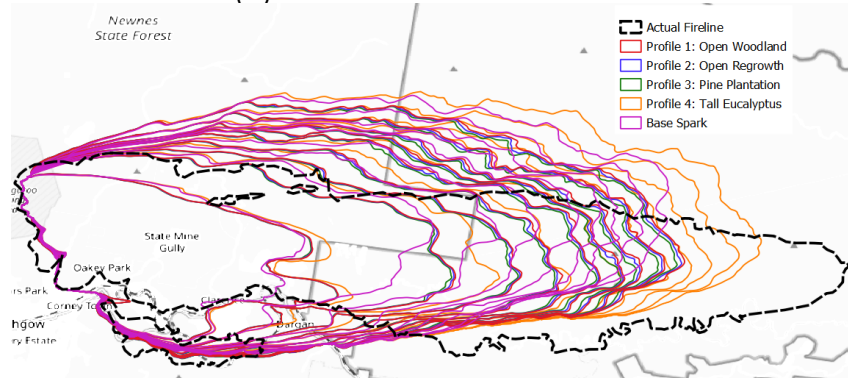
FIG. 7 KILMORE FIRE 2009 OF VICTORIA. THE BLACK DOTTED LINE REPRESENTS THE ACTUAL RECORDED FINAL FIRE PERIMETER.



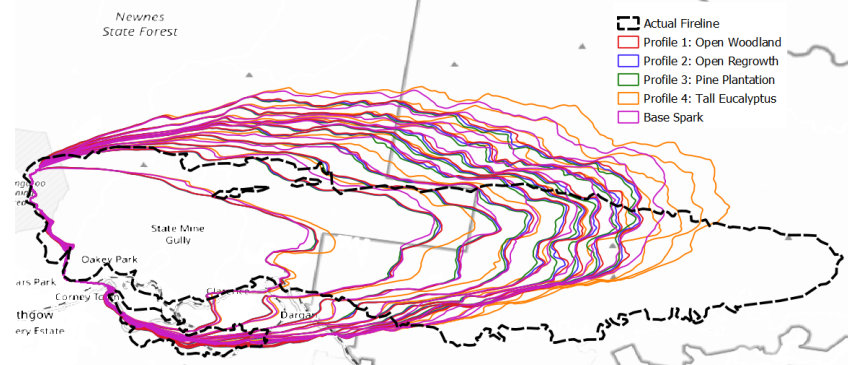
(a) Default WRF=1.0, PAI=LAI



(b) Default WRF=3.0, PAI=LAI

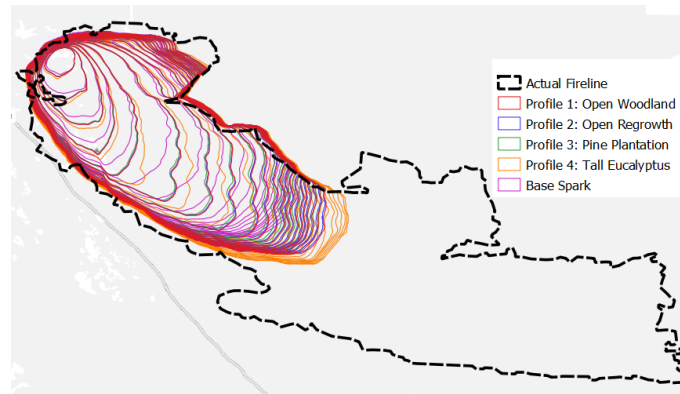


(c) Default WRF=1.0, PAI=LAI/2

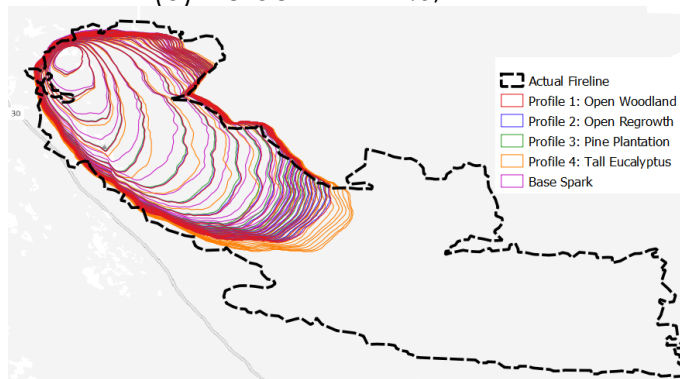


(d) Default WRF=3.0, PAI=LAI/2

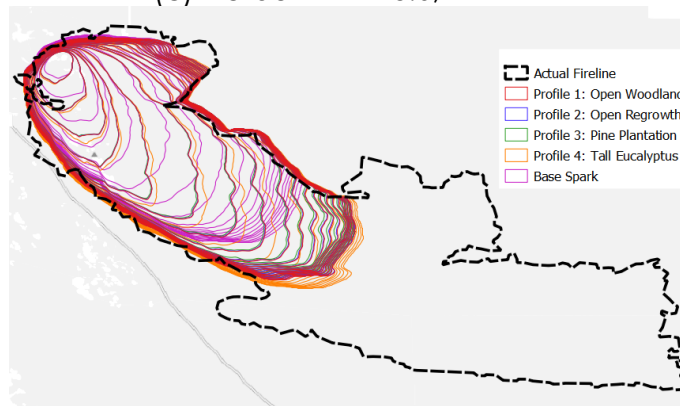
FIG. 8 LITHGOW FIRE 2013 OF NSW. THE BLACK DOTTED LINE REPRESENTS THE ACTUAL RECORDED FINAL FIRE PERIMETER.



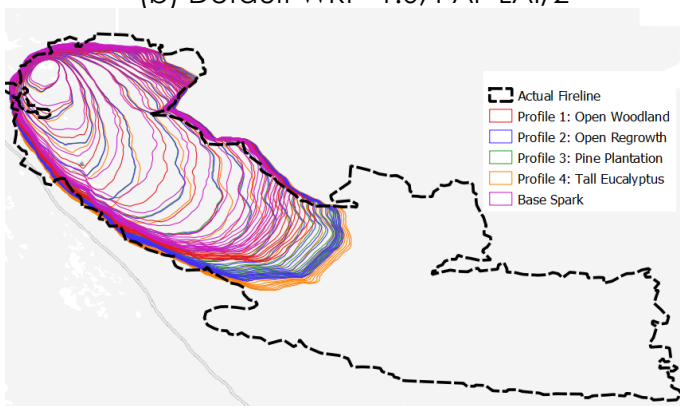
(a) Default WRF=1.0, PAI=LAI



(c) Default WRF=3.0, PAI=LAI



(b) Default WRF=1.0, PAI=LAI/2



(d) Default WRF=3.0, PAI=LAI/2

FIG. 9 MOUNT COOKE FIRE 2003 OF WA. THE BLACK DOTTED LINE REPRESENTS THE ACTUAL RECORDED FINAL FIRE PERIMETER.

In Figure 8, hourly fire perimeter lines are presented for the Lithgow fire. Results of the Lithgow fire simulations have shown a similar trend to the Kilmore fire. The



default WRF does not contribute to significant changes and  $PAI = LAI/2$  provides better results compared to  $PAI = LAI$  selection.

Hourly fire perimeter lines are presented for the Mount Cooke in Figure 9. The Mount Cooke fire results have behaved differently than the other two cases. All LAD based simulations outperformed the Base Spark regardless of the default WRFs and PAIs.

It can also be noted that among the LAD profiles, *Tall Open Eucalyptus* is again performing better than others for Lithgow and Mount Cooke fires. Swedosh et. al. [13] reported that in both Lithgow and Mount Cooke fires, burning occurred through a large area of dry eucalypt forest.



## CONCLUSIONS

In this study, we implemented a dynamic wind reduction factor (WRF) model which is based on a forest leaf area density (LAD) within the Vesta fire propagation model of Spark. This LAD-based WRF model is founded on a set of equations presented by Massman et al [6]. Initially, the model was tested using a set of synthetic data applying canopy parameters that represent Australian vegetation properties. Observing some variation in fire rate of spread comparing simulations with and without the Massman et. al. model, we assessed the implementation using three real case studies of near past fire occurrences in Australia: Mount Cooke Fire 2003 of Western Australia, Kilmore Fire 2009 of Victoria, and Lithgow Fire (State Mine) 2013 of New South Wales. Four different LAD configurations were tested: Open Woodland, Open Regrowth, Pine Plantation and Tall Open Eucalyptus. As plant area index (PAI) data is not publicly available, we tested  $PAI = LAI$  (leaf area index) and  $PAI = LAI/2$ . It is found that with Tall Open Eucalyptus and  $PAI = LAI/2$ , the best results are obtained in relation to the actual final fire perimeter. In all three cases, the dominant fuel was either Eucalyptus and/or understories.

To make regular use of the Massman et al model for operational purposes, PAI data for relevant areas needs to be collected and made available through *Landscape Data Visualiser* [8]. The model implementation also needs further calibration.



## REFERENCES

- 1 McArthur, A.G., *Fire behaviour in eucalypt forests*. 1967, Forestry and Timber Bureau, Australia.
- 2 Gould, J.S., et al., *Project Vesta: fire in dry eucalypt forest: fuel structure, fuel dynamics and fire behaviour*. 2008: Csiro Publishing.
- 3 Harman, I.N. and J.J. Finnigan, *A simple unified theory for flow in the canopy and roughness sublayer*. *Boundary-layer meteorology*, 2007. **123**(2): p. 339-363.
- 4 Moon, K., T. Duff, and K. Tolhurst. *Sub-canopy forest winds: understanding wind profiles for fire behaviour simulation*. *Fire Safety Journal*, 2016.
- 5 Sutherland, D., et al., *Large Eddy Simulation of Flow Over Streamwise Heterogeneous Canopies: Quadrant Analysis*. 2018.
- 6 Massman, W.J., J. Forthofer, and M.A. Finney, *An improved canopy wind model for predicting wind adjustment factors and wildland fire behavior*. *Canadian Journal of Forest Research*, 2017. **47**(5): p. 594-603.
- 7 Miller, C.a.H., James and Sullivan, Andrew and Prakash, Mahesh. *SPARK--A bushfire spread prediction tool*. in *International Symposium on Environmental Software Systems*. 2015. Springer.
- 8 TERN and ANU. *Landscape Data Visualiser (Downloadable Repository)*. 2019; Available from: <https://maps.tern.org.au/#/>.
- 9 Cruz, M.G., Sullivan, A. L., Gould, J. S., Sims, N. C., Bannister, A. J., Hollis, J. J., & Hurley, R. J., *Anatomy of a catastrophic wildfire: the Black Saturday Kilmore East fire in Victoria, Australia*. *Forest Ecology and Management*, 2012(284): p. 269-285.
- 10 Wikipedia. *2013 New South Wales bushfires*. 2013 [cited 2021 Jul].
- 11 Burrows, N.D., *Mt cooke wildfire january 2003: Monitoring impacts and recovery*. DBCA Library, Government of Western Australia, 2003.
- 12 Simard, M., et al., *Mapping forest canopy height globally with spaceborne lidar*. *Journal of Geophysical Research: Biogeosciences*, 2011. **116**(G4).
- 13 Swedosh, W., J. Hilton, and C. Miller, *Spark Evaluation – 0.9.7*. 2018, CSIRO: CSIRO. p. 42.